

Advanced Hemodynamic Modeling of Pulsatile Blood Flow with Magnetic Nano-particles: Fractional Analysis for Optimizing Biomedical Applications

*Azhar Ali Zafar, Muhammad Shahzaib, Khurram Shabbir
Department of Mathematics,
Government College University, Lahore, 54000, Pakistan

*Corresponding Author
azharalizafar@gcu.edu.pk

Received: 01 January, 2025 / Accepted: 11 February, 2025 / Published online: 16 July, 2025

Abstract. Hemodynamic analysis plays a crucial role in the prevention, diagnosis, and treatment of human vascular diseases. The use of magnetic particles in biomedicine and clinical therapies for targeted drug delivery within cells provides simple diagnostic tools. In this article we will study the periodic pulsatile blood flow in the femoral and coronary arteries using nano-particles. Based on experimental data regarding blood rheology, the study employs the constitutive equation of an Oldroyd-B fluid. Moreover to capture more control, the problem is modeled using the ABC fractional derivative operator and solved through the application of integral transforms. Furthermore, a comprehensive graphical analysis is conducted to understand the influence of the fractional order parameter and various material factors, such as amplitude, lead angle, frequency of body acceleration, magnetic field, particle concentration, and temperature effects, leading to significant conclusions. The obtained results help to optimize targeted drug delivery to infected tissues, and hyperthermia treatments.

AMS (MOS) Subject Classification Codes: 76A05;65N22;44A10;65Rxx;65L60.

Key Words: *ABC fractional derivative operator, Oldroyd-B fluid, Magnetohydrodynamics, Integral transform .*

1. Introduction

Biomagnetic fluid dynamics (BFD) is a specific subject of fluid dynamics that studies fluid flow in the presence of magnetic fields. Bio-magnetic-fluids (BMF) play a crucial part in bioengineering, particularly in applications such as magnetic drug delivery, enhancing blood flow during surgeries, treating cancerous tumours, regulating blood flow during medical procedures and transporting complex biological waste fluids. BFD is also crucial for the development of instruments for cell separation and endoscopy [33, 34, 23]. The human

blood circulatory system consists of a complex network of arteries and veins. Arteries are elastic vessels that transport oxygenated blood throughout the body. Their elasticity allows them to accommodate the volumetric changes necessary to move blood (an incompressible fluid), through the vascular system. Westerhof [48] proposed and modeled a simplified arterial network, comprising 55 major arteries in the human body, using electrical circuit analogies. Furthermore, the fluid properties that mimic blood, composed of blood plasma and RBCs, are adopted from a prior study [17]. Haik et al. [18] developed the concept of BMF within the human body. Specifically, BFD primarily addresses non-Newtonian viscous fluid flows, such as blood in arteries.

Variation in blood circulation can be caused by external acceleration. The body experiences acceleration forces during activities such as traveling at high speeds in vehicles and airplanes or making quick movements while playing sports. These forces can lead to headaches and an elevated heart rate. Prolonged exposure to such conditions may impair blood circulation, potentially causing vision loss. Therapeutic therapies and the creation of novel diagnostic instruments may benefit from controlled acceleration. Since blood is a BMF, its circulation can be optimized and regulated using external magnetic fields, potentially preventing heart issues [13].

A BFD model that was similar to ferro-hydrodynamics was developed in 1999 by Haik et al., further investigation related to the effects of magnetic fields on blood circulation was done by Tzirtzilakis [43], while studies on arteries with numerous stenoses were undertaken by Lundgren et al. [22] and Varshney and Kumar [46]. Unsteady flow of non-Newtonian fluids is influenced by the thermal variations [4]. Furthermore, the heat transfer characteristics and blood circulation in stenosed arteries were studied under a magnetic field by Bourhan and Magableh [9]. Moreover, Mustapha et al. [29] also made important contributions to this subject. The therapeutic value of magnetic particles in biomedicine has been recognised by numerous researchers that have explored blood mixed with magnetic particles in various geometries under the influence of magnetic fields. A blood circulation model with suspended magnetic particles along with magnetic field was used in Ali et al. [3] to analyse the therapeutic potential of magnetic particles. They observed that by controlling the magnetic field intensity suitably, the blood's and the particles' velocities could be controlled.

Grief et al. [16] studied the effect of a perpendicular magnetic field on blood flow, containing suspended magnetic particles, and concluded that the magnetic particles could increase the effectiveness of cancer therapy. Kilgus [20] observed that the addition of magnetic particles enhanced the model's ability to deliver targeted genes. In order to cure atherosclerosis and hypertension. Shit and Roy [39] developed a model that used magnetic particles in blood and demonstrated that blood flow could be controlled by an external magnetic field. Mirza et al. [28] studied the role of a magnetic field in treating stenosed arteries and observed significant changes in magnetized blood flow with suspended magnetic particles near the stenosed area. Further, Jawad et al. [19] investigated the computational study on MHD flow of nanofluid flow.

Blood closely resembles an Oldroyd-B fluid [31] due to its complex viscoelastic properties, which encompass both elasticity and viscosity. It consists of plasma, a Newtonian fluid, and suspended cellular components such as red blood cells (RBCs), white blood cells, and platelets. These elements collectively impart viscoelastic behavior to blood:

- Elasticity: RBCs deform and recover their shape, exhibiting elastic characteristics.
- Viscosity: Plasma contributes to the viscous properties of blood flow.

An Oldroyd-B fluid model is specifically designed to represent such viscoelastic behaviors, making it a more accurate representation of blood compared to purely Newtonian or other non-Newtonian models. Additionally, blood demonstrates stress relaxation, where stress diminishes over time under constant strain, and elastic memory, enabling it to revert to its original configuration. These properties align with the fundamental features of Oldroyd-B fluids, which incorporate memory effects in their constitutive equations. While bloods shear-thinning behavior (reduction in viscosity with increased shear rate) is often modeled using power-law [10] or Carreau models [11], its dynamic interaction of elastic and viscous properties across varying flow conditions aligns well with the predictive capabilities of the Oldroyd-B fluid framework. Furthermore, blood flows in pulsatile patterns within vessels due to the heart's pumping action. The Oldroyd-B model effectively captures the oscillatory shear stress response and the phase lag between stress and strain, which are hallmarks of blood flow. In microcirculation, where RBC deformation significantly impacts flow and resistance, an Oldroyd-B model provides a better representation of these deformation and relaxation effects than simpler Newtonian models.

More recently, fractional calculus (FC) has enabled the creation of more realistic and adaptable models that incorporate memory effects, displaying remarkable efficiency in controller design [27],[32],[21]. These benefits make FC modelling useful for developing active control schemes and linear state-feedback controllers to manage hyper-chaos [37]. For usefulness of fractional-order magnetohydrodynamic boundary layer fluid flow we refer the work of Sadiq and Hamasalh [36]. Furthermore, for the human liver, Baleanu et al. [8] suggested a fractional-order model (FOM). Furthermore, in the presence of a magnetic field, a FOM for blood flow was studied by Shah et al.[40] later by Riaz and Zafar [35]. Moreover, Zafar et al. [51] reported analytical results for two-phase blood flow in the presence of a magnetic field. Likewise, Maiti et al. in [30]investigates a FOM for blood flow with heat and mass transfer in the presence of thermal radiation. Recently, in [7] Awrejcewicz et al. investigate the blood rheology through the coronary and femoral arteries influenced by body acceleration.

Available literature indicates that blood acts as a Newtonian fluid at high shear rates, typically present in larger arteries, and displays non-Newtonian properties at low shear rates found in smaller arteries. Additionally, experimental data suggests that blood possesses viscoelastic characteristics under specific conditions [45, 12]. Thurston [41] was the first one to identify these viscoelastic properties, developing an extended Maxwell model for one-dimensional flow. Yeleswarapu et al. [42] and Yeleswarapu [50] proposed a three-parameter Oldroyd-B fluid model to study blood flow. Blood is known to be slightly viscoelastic, although most computational fluid dynamics studies have not taken this into consideration. An aggregate of red blood cells exhibits solid-body behavior and the capacity to store elastic energy at low shear rates. However, viscoelastic effects become less noticeable at high shear rates because of the fluid-like behavior of red blood cells. Consequently, blood flow under oscillatory flow conditions and at low shear stress is better represented by viscoelastic models [49].

For simulating a mathematical model there are several methods depending upon the nature

of problem for instance CrankNicolson finite-difference scheme [5], [6]. Sometimes, integral transform methods seems to be more useful.

While traditional studies on blood models have predominantly treated blood as a Newtonian fluid, there has been limited exploration of non-Newtonian fluid models using FC. Addressing this gap, our manuscript focuses on developing a blood flow model for a specific category of non-Newtonian fluids with fractional order (FO) derivatives, incorporating uniformly distributed magnetic nanoparticles (NP) as the blood flows through coronary and femoral arteries. By adjusting parameters in the governing equation of the model, for instance, setting the λ_2 retardation parameter to zero results in blood behavior analogous to a Maxwell fluid, while a zero value for the λ_1 relaxation parameter reverts the model to a Newtonian fluid. This flexibility allows for a generalized modeling approach. The Laplace transform (LT) method and well known Stehfest's numerical inversion algorithm (SNIA) [38] are employed to solve the model under the given initial and boundary conditions. Our research also extends to the application of magnetic particles in biomedical and clinical therapies, which has become a focal point of interest in recent years. This study presents a mathematical model of two-phase unsteady pulsatile blood flow in femoral and coronary arteries, incorporating suspended NP, body acceleration, and an external magnetic field, alongside heat transfer effects. More precisely:

- a:** Our aim is to investigate a time-fractional model for blood rheology (regarded as an Oldroyd-B fluid) containing uniformly dispersed magnetic NP passing through the coronary and femoral arteries.
- b:** This dimensionless form model accounts for the effects of fractional order parameters, an external magnetic field, periodic body acceleration, and an oscillating pressure gradient.
- c:** Specifically, the Atangana-Baleanu (ABC) time fractional derivatives will be utilized to model the problem, as the ABC derivative provides superior results for problems involving heat transfer.
- d:** The LT method, FHT and SNIA are employed to simulate the model subject to given constraints.
- e:** Numerous results from the literature can be retrieved and replicated from our general solutions by suitably adjusting the parameters and functions. Consequently, the challenges linked to analogous models will be thoroughly resolved.
- f:** A comprehensive parametric analysis is performed through graphical methods, yielding valuable insights that contribute to process optimization and the advancement of innovative medical technologies.

1.1. Research Design. Our methodological approach begins with an overview of existing research and the motivation behind the study. In Section 2, the mathematical model of the proposed problem is formulated in its dimensional form, with governing equations expressed as partial differential equations (PDEs) under appropriate constraints. In Section 3, the system of equations is transformed into a dimensionless form, and a non-integer order model is developed using the ABC non-integer order derivative operator. Section 4 presents the solution to the mathematical model, achieved through the application of integral transforms (specifically the LT and FHT), along with Stehfests algorithm for the inverse LT. The validation of the obtained results is addressed in Section 5. A detailed graphical analysis

of the results is provided in Section 6, followed by a discussion. Finally, conclusions and remarks are presented in Section 7, with future directions outlined in Section 8.

2. MATHEMATICAL FRAMEWORK OF THE PROBLEM

The study considers blood, modeled as an Oldroyd-B fluid, flowing through an artery represented as a cylindrical glass tube with a radius r_0 . This tube contains uniformly distributed magnetic NP, specifically iron oxide. The flow is directed along the z -axis and is influenced by a magnetic field, periodic body acceleration, and an axial pulsatile pressure gradient. The physical geometry of the problem is shown in figure 1. The primary focus

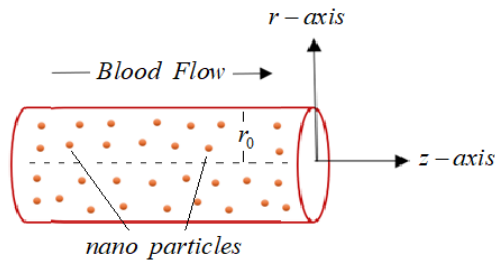


FIGURE 1. Physical geometry of the fluid flow.

of this investigation is the non-Newtonian blood flow through the femoral and coronary arteries. Typically, coronary arteries have an average diameter of approximately 3.1 mm, while femoral arteries generally range in diameter from 3.9 mm to 8.9 mm.

Our presumptions are as follows:

- The blood and magnetic particles exhibit zero velocity at the artery walls, complying with the no-slip requirement.
- The induced magnetic field has a minor effect since the magnetic Reynolds number is kept low.
- Blood's physical characteristics, such as its density and viscosity, never change.
- The blood volume has an even distribution of magnetic NP.

The blood and magnetic NP are both still at $t = 0$. The fluid with suspended particles begins to move shortly after $t = 0$, driven by an oscillating pressure gradient and convective heat transfer. Newton's second law defines particle motion, while the Navier-Stokes equation governs fluid motion. The electromagnetic field's behaviour is determined by Maxwell's equations.

The momentum equation of fluid stream is [30], [7].

$$\begin{aligned} & \left(1 + \lambda_1 \frac{\partial}{\partial t}\right) \frac{\partial V_f(r, t)}{\partial t} = - \left(1 + \lambda_1 \frac{\partial}{\partial t}\right) \frac{1}{\rho} \frac{\partial p(r, t)}{\partial z} + \left(1 + \lambda_1 \frac{\partial}{\partial t}\right) B_a \\ & + \left(1 + \lambda_2 \frac{\partial}{\partial t}\right) \left(\frac{\partial^2 V_f(r, t)}{\partial r^2} + \frac{1}{r} \frac{\partial V_f(r, t)}{\partial r} \right) - \left(1 + \lambda_1 \frac{\partial}{\partial t}\right) \frac{SN}{\rho} (V_f(r, t) - V_p(r, t)) \\ & - \left(1 + \lambda_1 \frac{\partial}{\partial t}\right) \frac{\sigma B_{app}^2}{\rho} V_f(r, t) + \left(1 + \lambda_1 \frac{\partial}{\partial t}\right) g \beta_{T_f} (T_f(r, t) - T_{f\infty}(r, t)), \end{aligned} \quad (2. 1)$$

where λ_1 is relaxation time parameter, V_f denotes velocity of fluid, $\frac{\partial p}{\partial z}$ is the pressure gradient along the flow direction, B_a denotes the body acceleration, λ_2 is the retardation time parameter, S is Stoke's constant, N denotes the number of magnetic particles per unit volume, V_p is the velocity of particles, σ is the electric conductivity, B_{app} strength of applied magnetic field, T_f denotes temperature of fluid, β_{T_f} is the thermal expansion coefficient and $T_{f\infty}$ is the ambient temperature. All other nomenclature is declared in Table 1. Considering small values of Reynolds number for relative velocities, the net force

TABLE 1. Nomenclature

Symbol	Quantity	Symbol	Quantity
α	Fractional parameter	β, γ	Fractional parameters
a	Womersley number	q	Laplace transform parameter
ψ_0	Constant amplitude	ϕ	Lead angle
ψ_1	Pulsatile component's amplitude	ω_r	Frequency of body acceleration
m_{av}	Average mass of magnetic particles	Ha	Hartman number
μ	Viscosity (Dynamic)	G_r	Grashof Number
ν	Viscosity (Kinematic)	A_g	Amplitude
c_p	Specific heat at constant pressure	k	coefficient of thermal conductivity

acting on fluid depends linearly on their relative velocities of blood and suspended magnetic NPs, therefore

$$m_{av} \frac{\partial V_p(r, t)}{\partial t} = S(V_f(r, t) - V_p(r, t)). \quad (2. 2)$$

Moreover, energy equation is given as

$$\rho c_p \frac{\partial T_f(r, t)}{\partial t} = k \left(\frac{\partial^2 T_f(r, t)}{\partial r^2} + \frac{1}{r} \frac{\partial T_f(r, t)}{\partial r} \right). \quad (2. 3)$$

Like in [25] $\frac{\partial p}{\partial z}$ is considered as

$$-\frac{\partial p}{\partial z} = \psi_0 - \psi_1 \cos(\omega_p t), \quad (2. 4)$$

where ψ_0 represents the constant amplitude of pressure gradient, while ψ_1 denotes the amplitude of pulsatile component of pressure gradient which give rise to systolic and diastolic pressure gradient, $p_\omega = 2\pi p_f$ with p_f is the pulse frequency. The approximate value of ψ_0 is $32 \times 10^{-3} Nm^{-1}$ for femoral and subsequently $698.65 \times 10^{-3} Nm^{-1}$ for coronary

arteries (for details see [15], [26]). Expression for the body acceleration along the axial-direction is determine by

$$B_a = A_g \cos(\omega_b t + \theta), \quad (2.5)$$

where A_g represents amplitude, θ is the lead angle with regarding cardiac activity and ω_b is frequency for body acceleration.

The associated constraints for the problem are:

$$V_f(r, 0) = V_p(r, 0) = 0, \quad T_f(r, 0) = T_{f\infty}, \quad \text{at } t = 0 \text{ and } r > 0, \quad (2.6)$$

$$\frac{\partial V_f(r, t)}{\partial r} = 0, \quad \frac{\partial T_f(r, t)}{\partial r} = 0, \quad \text{at } r = 0 \text{ and } t > 0, \quad (2.7)$$

$$V_f(r, t) = V_p(r, t) = 0, \quad T_f(r, t) = T_{fw}, \quad \text{at } r = r_0 \text{ and } t > 0. \quad (2.8)$$

3. NON-DIMENSIONALIZATION AND FRACTIONAL ANALOGUE OF THE PROBLEM

To make the problem under consideration geometry free, the following dimensionless quantities are introduced:

$$r^* = \frac{r}{r_0}, \quad t^* = \frac{w_p t}{2\pi}, \quad V_f^* = \frac{V_f}{V_0}, \quad V_p^* = \frac{V_p}{V_0}, \quad T_f^* = \frac{T_f - T_{f\infty}}{T_{fw} - T_{f\infty}}. \quad (3.9)$$

The dimensionless system of coupled partial DEs after dropping '*' becomes

$$\begin{aligned} & \left(1 + \lambda_1 \frac{\partial}{\partial t}\right) \frac{a^2 \partial V_f(r, t)}{2\pi \partial t} = \left(1 + \lambda_1 \frac{\partial}{\partial t}\right) \chi_1 (1 + e \cos(2\pi t)) + \\ & \left(1 + \lambda_1 \frac{\partial}{\partial t}\right) \chi_2 \cos(2\pi \omega_r t + \theta) + \left(1 + \lambda_2 \frac{\partial}{\partial t}\right) \left(\frac{\partial^2 V_f(r, t)}{\partial r^2} + \frac{1}{r} \frac{\partial V_f(r, t)}{\partial r} \right) - \\ & \left(1 + \lambda_1 \frac{\partial}{\partial t}\right) R (V_f(r, t) - V_p(r, t)) - \left(1 + \lambda_1 \frac{\partial}{\partial t}\right) H a^2 V_f(r, t) + \left(1 + \lambda_1 \frac{\partial}{\partial t}\right) G_r T_f(r, t), \end{aligned} \quad (3.10)$$

$$M \frac{\partial V_p(r, t)}{\partial t} = V_f(r, t) - V_p(r, t), \quad (3.11)$$

$$\frac{\partial T_f(r, t)}{\partial t} = \frac{1}{P_r} \left(\frac{\partial^2 T_f(r, t)}{\partial r^2} + \frac{1}{r} \frac{\partial T_f(r, t)}{\partial r} \right). \quad (3.12)$$

Moreover, the initial and boundary conditions associated with the fluid flow model in dimensionless relations are:

$$V_f(r, t) = 0, \quad T_f(r, t) = 0, \quad \text{at } r = 0, \quad t > 0, \quad (3.13)$$

$$\frac{\partial V_f(r, t)}{\partial r} = 0, \quad \frac{\partial T_f(r, t)}{\partial r} = 0, \quad \text{at } r = 0, \quad t \geq 0, \quad (3.14)$$

$$V_f(r, t) = 0, \quad V_p(r, t) = 0, \quad T_f(r, t) = 1, \quad \text{at } r = 1, \quad t > 0, \quad (3.15)$$

where $a^2 = \frac{\rho \omega_p r_0^2}{\mu}$, $\chi_1 = \frac{\psi_0 r_0^2}{\mu u_0}$, $e = \frac{\psi_1}{\psi_0}$, $\chi_2 = \frac{\rho A_g r_0^2}{\mu u_0}$, $\omega_r = \frac{\omega_b}{\omega_p}$, $H a^2 = B_0^2 \frac{\sigma}{\mu}$, $R = \frac{S N r_0^2}{\mu}$ and $M = \frac{m_{av} \mu}{\rho r_0^2 S}$.

Here, a is a dimensionless parameter known as the Womersley number [47], which expresses the relationship between pulsatile flow frequency and viscous effects. This number is critical for preserving dynamic similarity when scaling experiments. It is used to scale up the vascular system for experimental investigations due to its potent effects. The Womersley number is a dimensionless parameter crucial in hemodynamics, as it measures the relative influence of unsteady (oscillatory) inertial forces compared to viscous forces in pulsatile blood flow. It plays a key role in understanding blood flow dynamics across different regions of the circulatory system.

At low Womersley numbers (less than unity): Viscous forces dominate, resulting in parabolic flow profiles resembling steady laminar flow, typically observed in small vessels such as capillaries.

At high Womersley numbers (greater than 10): Inertial forces take precedence, leading to flatter velocity profiles and wave-like flow propagation, characteristic of large arteries like the aorta.

At intermediate values (between 1 and 10): A combination of viscous and inertial effects leads to pronounced velocity oscillations throughout the cardiac cycle.

The Womersley number also describes how the oscillatory nature of blood flow, driven by the hearts pumping action, interacts with vessel walls and the viscous properties of blood. This parameter provides valuable insights into the behaviour of pulsatile blood flow under various conditions, enhancing our understanding of cardiovascular physiology and supporting the development of diagnostic and therapeutic approaches.

As we have obtained our model equations (10)-(15) in dimensionless form, the equivalent non-inter order model is obtained by exchanging time derivative terms by the ABC-non-integer order derivative operator, hence

$$\frac{a^2}{2\pi}(1 + \lambda_1 D_t^\alpha)V_f(r, t) = (1 + \lambda_1 D_t^\alpha)\chi_1(1 + e\cos(2\pi t)) + (1 + \lambda_1 D_t^\alpha)\chi_2\cos(2\pi\omega_r t + \theta) \quad (3. 16)$$

$$+ (1 + \lambda_2 D_t^\beta) \left(\frac{\partial^2 V_f(r, t)}{\partial r^2} + \frac{1}{r} \frac{\partial V_f(r, t)}{\partial r} \right) - (1 + \lambda_1 D_t^\alpha)R(V_f(r, t) - V_p(r, t)) \\ - (1 + \lambda_1 D_t^\alpha)Ha^2 V_f(r, t) + (1 + \lambda_1 D_t^\alpha)G_r T_f(r, t),$$

$$MD_t^\alpha V_p(r, t) = V_f(r, t) - V_p(r, t), \quad (3. 17)$$

$$D_t^\gamma T_f(r, t) = \frac{1}{p_r} \left(\frac{\partial^2 T_f(r, t)}{\partial r^2} + \frac{1}{r} \frac{\partial T_f(r, t)}{\partial r} \right), \quad (3. 18)$$

where $\alpha, \beta, \gamma \in (0, 1)$ and $D_t^\delta(\cdot)$ is the ABC-non-integer order derivative operator [2] defined as

$$D_t^\delta h(t) = \frac{1}{(1 - \delta)} \int_0^t h'(\tau) E_\delta \left[\frac{\delta}{1 - \delta} (t - \tau)^\delta \right] d\tau, \quad \delta \in (0, 1), \quad (3. 19)$$

and $\frac{1}{1-\delta}E_\delta \left[-\frac{\delta}{1-\delta}t^\delta \right]$ is the kernel of the derivative operator with $E_\delta(\cdot)$ is the well celebrated Mittag-Leffler function [1]. Furthermore, the LT of the FO ABC operator is:

$$L(D_t^\delta h(t)) = \frac{q^\delta L\{h(t)\}}{(1-\delta)q^\delta + \delta} - \frac{q^{\delta-1}h(0)}{(1-\delta)q^\delta + \delta}. \quad (3.20)$$

4. COMPUTATIONAL FRAMEWORK

In this section, we will simulate our model governing equations by employing the integral transforms. Moreover, it is important to note that in order to solve the momentum equation we need to find the solution for temperature. Therefore first we will solve Eq. (18) and then use it in the solution of Eqs. (16) and (17)

4.1. Computation for the Temperature Profile. The equation derived by applying Laplace Transform (LT) [14] to Eq. (18) is

$$\frac{q^\gamma}{(1-\gamma)q^\gamma + \gamma} \tilde{T}_f(r, q) = \frac{1}{P_r} \left(\frac{\partial^2 \tilde{T}_f(r, q)}{\partial r^2} + \frac{1}{r} \frac{\partial \tilde{T}_f(r, q)}{\partial r} \right), \quad (4.21)$$

along with

$$\tilde{T}_f(1, q) = \frac{1}{q}. \quad (4.22)$$

Applying finite Hankel transform (FHT) [14] to Eq(21) yields

$$\tilde{T}_{Hf}(r_n, q) = \frac{J_1(r_n)}{r_n} \frac{1}{q} - \frac{a_{5n} J_1(r_n)}{r_n q^\gamma + a_{4n}}. \quad (4.23)$$

Employing inverse LT, we get

$$T_{Hf}(r_n, t) = \frac{J_1(r_n)}{r_n} - \frac{J_1(r_n)}{r_n} F_\gamma(-a_4, t), \quad (4.24)$$

where $L^{-1} \left\{ \frac{1}{(q^a - c)} \right\} = \sum_{n=0}^{\infty} \frac{c^n t^{(n+1)a}}{\Gamma(n+1)a}$: is Robotnov and Hartley function [24].

Taking the inverse FHT [14] of Eq. (25) yields the following equation:

$$T_f(r, t) = 1 - 2 \sum_{n=0}^{\infty} \frac{a_{5n} J_0(r r_n)}{r_n J_1(r_n)} F_\gamma(-a_{4n}, t), \quad (4.25)$$

$$a_0 = \frac{1}{1-\gamma}, a_1 = a_0 \gamma, a_2 = \frac{a_0}{b_0}, b_0 = \frac{1}{P_r}, a_{3n} = a_2 + r_n^2, a_{4n} = \frac{a_1 r_n^2}{a_{3n}}, a_{5n} = \frac{a_2}{a_2 + r_n^2}.$$

4.2. Computation for the Velocity Profile. Applying Laplace transform [14] to Eq.(16), we get:

$$\begin{aligned} \frac{a^2}{2\pi} \left(q + \lambda_1 \frac{q^{\alpha+1}}{(1-\alpha)q^\alpha + \alpha} \right) \tilde{V}_f(r, q) &= \left(1 + \lambda_1 \frac{q^\alpha}{(1-\alpha)q^\alpha + \alpha} \right) \chi_1 \left(\frac{1}{q} + e \frac{q}{q^2 + (2\pi)^2} \right) + \\ &\left(1 + \lambda_1 \frac{q^\alpha}{(1-\alpha)q^\alpha + \alpha} \right) \chi_2 \left(\cos(\phi) \frac{q}{q^2 + (2\pi\omega_r)^2} + \sin(\phi) \frac{2\pi\omega_r}{q^2 + (2\pi\omega_r)^2} \right) + \\ &\left(1 + \lambda_2 \frac{q^\beta}{(1-\beta)q^\beta + \beta} \right) \left(\frac{\partial^2 \tilde{V}_f(r, q)}{\partial r^2} + \frac{1}{r} \frac{\partial \tilde{V}_f(r, q)}{\partial r} \right) - \left(1 + \lambda_1 \frac{q^\alpha}{(1-\alpha)q^\alpha + \alpha} \right) R(\tilde{V}_f(r, q) - \\ \tilde{V}_p(r, q)) &- \left(1 + \lambda_1 \frac{q^\alpha}{(1-\alpha)q^\alpha + \alpha} \right) Ha^2 \tilde{V}_f(r, q) + \left(1 + \lambda_1 \frac{q^\alpha}{(1-\alpha)q^\alpha + \alpha} \right) G_r \tilde{T}_f(r_n, q), \end{aligned} \quad (4.26)$$

Applying FHT [14]

$$\frac{a^2}{2\pi} \left(1 + \lambda_1 \frac{q^\alpha}{(1-\alpha)q^\alpha + \alpha} \right) \tilde{V}_f(r_n, q) = \frac{J_1(r_n)}{r_n} \left(1 + \lambda_1 \frac{q^\alpha}{(1-\alpha)q^\alpha + \alpha} \right) \left[\chi_1 \left(\frac{1}{q} + e \frac{q}{q^2 + (2\pi)^2} \right) + \right. \quad (4.27)$$

$$\left. \chi_2 \left(\cos(\phi) \frac{q}{q^2 + (2\pi\omega_r)^2} + \sin(\phi) \frac{2\pi\omega_r}{q^2 + (2\pi\omega_r)^2} \right) \right] + \left(1 + \lambda_2 \frac{q^\beta}{(1-\beta)q^\beta + \beta} \right) (-r_n) V_f(r_n, q) + \\ \left(1 + \lambda_1 \frac{q^\alpha}{(1-\alpha)q^\alpha + \alpha} \right) R(\tilde{V}_f(r_n, q) - \tilde{V}_p(r_n, q)) - \left(1 + \lambda_1 \frac{q^\alpha}{(1-\alpha)q^\alpha + \alpha} \right) Ha^2 \tilde{V}_f(r_n, q) + \\ \left(1 + \lambda_1 \frac{q^\alpha}{(1-\alpha)q^\alpha + \alpha} \right) G_r \tilde{T}_f(r_n, q),$$

$$\tilde{V}_f(r_n, q) = \quad (4.28)$$

$$= \left[\frac{(x_{31}q^{+\beta} + x_{33})q^{2\alpha} + (x_{32}q^\beta + x_{34})q^\alpha + x_{35}q^\beta + x_{36}}{(x_{21}q + x_{22})q^{3\alpha} + (x_{23}q + x_{1n}q^\beta + x_{4n})q^{2\alpha} + (x_{25}q + x_{5n})q^\alpha + x_{27}q + x_{3n}q^\beta + x_{27}} \right] \\ \left[\chi_1 \left(\frac{1}{q} + e \frac{q}{q^2 + (2\pi)^2} \right) + \chi_2 \left(\cos(\phi) \frac{q}{q^2 + (2\pi\omega_r)^2} + \sin(\phi) \frac{2\pi\omega_r}{q^2 + (2\pi\omega_r)^2} \right) \right] \frac{J_1(r_n)}{r_n},$$

where,

$$\begin{aligned} a_{11} &= \frac{a}{2\pi}, x_{11} = a_{11}M + (1-\alpha), x_{12} = (Ha^2M + RM + Ha^2(1-\alpha)), x_{13} = \\ a_{11}\alpha, x_{14} &= Ha^2\alpha, x_{21} = ((1-\alpha) + \lambda_1)(1-\beta), x_{22} = ((1-\alpha) + \lambda_1)(1-\beta)x_{13}, x_{23} = \\ ((1-\alpha) + \lambda_1)(1-\beta)x_{13} &+ (1-\beta)x_{11}\alpha + ((1-\alpha) + \lambda_1)\beta x_{11}, x_{24} = (1-\beta)x_{12}\alpha + ((1-\alpha) + \\ \lambda_1)\beta x_{12}, x_{25} &= ((1-\alpha) + \lambda_1)(\beta)x_{13} + (1-\beta)x_{13}\alpha + \beta x_{11}\alpha, x_{26} = ((1-\alpha) + \lambda_1)x_{14} + \\ x_{14}(1-\beta)\alpha &+ \beta x_{12} + \beta x_{12}\alpha, x_{27} = \beta\alpha x_{13}, x_{14}\alpha, x_{31} = M + (1-\alpha)((1-\alpha) + \lambda_1), x_{32} = \\ (M + (1-\alpha)) &((1-\beta)\alpha + \alpha^2(1-\beta)((1-\alpha) + \lambda_1)\lambda_1), x_{33} = (M + (1-\alpha))\beta((1-\alpha) + \\ \lambda_1), x_{34} &= \alpha\beta(M + (1-\alpha)) + \alpha\beta((1-\alpha) + \lambda_1), x_{35} = (1-\beta)\alpha^2, x_{36} = \alpha^2\beta, x_{2n} = \\ (((1-\beta)\lambda_2(1-\alpha)(M &+ (1-\alpha)))r_n^2, x_{3n} = (((1-\beta) + \lambda_2)(\alpha(1-\alpha) + \alpha(M + \\ (1-\alpha))))r_n^2, &x_{4n} = ((1-\beta) + \lambda_2)r_n^2\alpha^2, x_{5n} = r_n^2\beta(1-\alpha)(M + (1-\alpha)), x_{6n} = \\ r_n^2\beta(\alpha(1-\alpha) &+ \alpha(M + (1-\alpha))), x_{7n} = r_n^2\alpha^2\beta, x_{8n} = x_{26} + x_{6n}, x_{9n} = x_{28} + x_{6n}. \end{aligned}$$

The desired results in the time domain can be determined by applying the inverse Laplace Transform to these expressions and in our case it is admittedly laborious. So, we apply SNIA to these expressions. SNIA for Laplace inversion is defined as [38]

$$L^{-1}\{\tilde{V}_f(r, q)\} = V_f(t) = ln2^{\frac{1}{i}} \sum_{j=1}^{2l} (-1)^{j+l} \sum_{m=\frac{j+1}{2}}^{\min(j,l)} \frac{m^l (2m)!}{(l-m)!m!(m-1)!(j-m)!(2m-j)!} \tilde{V}_f\left(ln2^{\frac{1}{i}}\right). \quad (4. 29)$$

For computing velocity of magnetic particles, taking the LT [14] of Eq. (17), we have

$$M \frac{q^\alpha}{(1-\alpha)q^\alpha + \alpha} \tilde{V}_p(r, q) = (\tilde{V}_f(r, q) - \tilde{V}_p(r, q)), \quad (4. 30)$$

$$\tilde{V}_p(r, q) = \left(\frac{(1-\alpha)q^\alpha + \alpha}{(M + (1-\alpha)q^\alpha + \alpha)} \right) \tilde{V}_f(r, q). \quad (4. 31)$$

Applying FHT [14], we get

$$\tilde{V}_p(r_n, q) = \left(\frac{(1-\alpha)q^\alpha + \alpha}{(M + (1-\alpha)q^\alpha + \alpha)} \right) \tilde{V}_f(r_n, q), \quad (4. 32)$$

$$\tilde{V}_p(r_n, q) = \left[\frac{1}{M_a} \frac{q^\alpha}{q^\alpha + M_b} + M_b \frac{1}{q^\alpha + M_b} \right] \tilde{V}_f(r_n, q). \quad (4. 33)$$

Applying inverse LT [14], we get

$$V_p(r, t) = \left[\frac{1}{M_a} R_{\alpha, -\alpha} \left(-\frac{1}{M_b}, t \right) + \frac{1}{M_b} F_\alpha \left(-\frac{1}{M_b}, t \right) \right] * V_f(r_n, t). \quad (4. 34)$$

Applying the inverse FHT [14], we get

$$V_p(r, t) = \left[\frac{1}{M_a} R_{\alpha, -\alpha} \left(-\frac{1}{M_b}, t \right) + \frac{1}{M_b} F_\alpha \left(-\frac{1}{M_b}, t \right) \right] * V_f(r, t). \quad (4. 35)$$

where $M_a = 1 + Ma_0$, $M_b = \frac{a_1}{M_a}$.

5. VALIDATION OF OBTAINED RESULTS

Our results in the limiting case when α, β approaches unity, $\lambda_1 = 0, \lambda_2 = 0$ and $G_r = 0$ are displayed in Fig.2. It is found that our results exhibit a satisfying consistency with the existing findings of Awrejcewicz et al. [7]. This obviously corroborates the validity of our model and further strengthens the utility of our obtained results. Moreover, as special or limiting case when α and β approaches unity, the Oldroyd-B fluid reduces to its classical model. Furthermore, when $\lambda_2 = 0$, obtained results are reduced to analogous fractional Maxwell model. Additionally, when both $\lambda_1 = 0$ and $\lambda_2 = 0$, this model behaves as a Newtonian fluid. Thus, corresponding results from the established works can be readily derived from our comprehensive results.

6. GRAPHS AND DISCUSSION

Hemodynamic analysis plays a crucial role in the prevention, diagnosis, and treatment of human vascular diseases. The use of magnetic particles in biomedicine and clinical therapies for targeted drug delivery within cells provides simple diagnostic tools. In this article we have studied the periodic pulsatile blood flow in the femoral and coronary arteries using nano-particles. Moreover to capture more control, the problem is modeled using the ABC fractional derivative operator and solved through the application of integral transforms. Furthermore, in this section a comprehensive graphical analysis is conducted to understand the influence of the fractional order parameter and various material factors, such as amplitude, lead angle, frequency of body acceleration, magnetic field, particle concentration, and temperature effects, leading to significant conclusions. Additionally, graphical analysis is performed to analyze the flow behavior using some fixed values of parameters (where not mentioned) such as $\alpha = 0.7, \beta = 0.7, \gamma = 0.7, w_r = 0.2$, amplitude $A_g = 0.5$, lead angle $\theta = 0$, relaxation time parameter $\lambda_1 = 0.5$, retardation time parameter $\lambda_2 = 0.5$, Prandtl number $P_r = 2$, particles concentration parameter $R = 4$, Hartman number $Ha = 4$ and Grashof Number $G_r = 5$. It is pertinent to mention that the range of the chosen parameter for graphical analysis is considered from the experimental study carried out in [42], [44] and [38].

(a) Influence radial parameter

Figures 3(a) and 3(b) depict velocities in the femoral and coronary arteries, respectively. It has been shown that the central artery has the highest magnetic and fluid particle velocities. This is explained by the fact that due to no slip at the walls of artery results in lowering the blood flow near the walls than along the axis. The velocity of magnetic particles follows a similar trend. Furthermore, it has been determined that the coronary artery has a greater blood and magnetic NP flow velocities than the femoral artery.

(b) Influence A_g and ω_r

Figures 4(a) and 4(b) show velocity profiles against time for the coronary and femoral arteries, respectively, with varying A_g at $r = 0$. It is shown that raising A_g leads to the faster motion of blood and magnetic particles. Figures 5(a) and 5(b) indicate that blood velocity decreases with increasing ω_r .

(c) Influence of lead angle θ

Figures 6(a) and 6(b) show velocity profiles over time for various lead angle θ values at $r = 0$. Compared to the coronary artery, where blood velocities decrease as the lead angle increases, the femoral artery exhibits a more pronounced effect of the lead angle on blood velocity.

(d) Influence of fractional parameter α and β

The control of the non-integer order parameters α and β on the velocity fields are seen in Figures 7(a) – 7(b) and 8(a) – 8(b). These curves show unique behaviour known as the memory effect that is not captured by classical derivatives and are produced at a fixed period. The fractional parameter α behaves differently at larger and smaller times as shown in Figures 7(a) and 7(b). Additionally, it is noted that the coronary artery has a comparatively higher blood and magnetic particle flow velocity than the femoral artery. The curves that are obtained will assist the researchers and experimentalists for curve fitting using data

from their experiments. Physically, at the middle of the artery, increasing α values causes the fluid's thermal conductivity to rise and its viscosity to drop for short periods of time, but over long periods, the effects reverse. Figures 8(a) and 8(b) illustrate velocity profiles versus radius for the coronary and femoral arteries, respectively, for various values of β at $t = 0.2$ and $t = 2$. Results have shown that increasing β causes the blood and magnetic particles to flow at lower velocities.

(e) *Influence of fractional parameter γ*

The effects of the non-integer order parameter γ on the velocity fields and temperature are illustrated in figures 9 and 10. These curves reveal unique behaviors, known as the memory effect, that are not captured by classical derivatives and occur at specific intervals. The fractional parameter γ exhibits opposite behaviors at larger and smaller times.

Figures 9(a) and 9(b) show integral curves and solutions that are not comprehensible in non FO models. Additionally, the coronary artery shows a comparatively higher blood and magnetic particle flow velocity than the femoral artery. These curves will assist experimentalists in fitting data from their experiments.

Figure 10 depicts temperature profiles against the radius for multiple values of γ at $t = 0.2$ and $t = 2$. Analysis reveals that increasing gamma results in lower temperatures at $t = 0.2$, while an opposite trend is seen at $t = 2$.

(f) *Influence of Hartman number Ha , particle concentration parameter R and Grashof Number G_r*

Figures 11(a) and 11(b) show how the magnetic parameter impacts velocity profiles; increasing magnetic parameter values causes the fluid velocity to drop significantly. This is physically conceivable because the transverse magnetic field generates a Lorentz drag force, which opposes the bulk flow and reduces longitudinal velocity. Figures 12(a) and 12(b) demonstrate how the particle mass and particle concentration parameters influence particle and blood velocities. They indicate a trend for velocities to decrease with rising R . Higher particle concentrations cause more collisions, scattering particles off streamlines and wasting energy, slowing the flow. Figures 13(a) and 13(b) show velocity profiles vs radius for various values of G_r at $t = 0.2$ and $t = 2$. Results indicate that increasing the Grashof number G_r results in higher velocities. Additionally, it has been determined that the coronary artery exhibits a significantly greater blood and magnetic particle flow velocity compared to the femoral artery.

(g) *Influence of relaxation time parameter λ_1 , retardation time parameter λ_2*

Figures 14 and 15 show the influence of λ_1 and λ_2 (the Oldroyd-B fluid parameters) on the velocity distribution. The figures make it evident that as λ_1 increases, the velocity profile ascends as well. This is because the fluid accelerates due to the rapid response of shear forces, and λ_1 is the time relaxation parameter. On the other hand, because of the shear stress delay reaction, a higher value of λ_2 results in a decreased velocity distribution. Furthermore, it is observed that the coronary artery has a comparatively higher blood and magnetic particle flow velocity than the femoral artery.

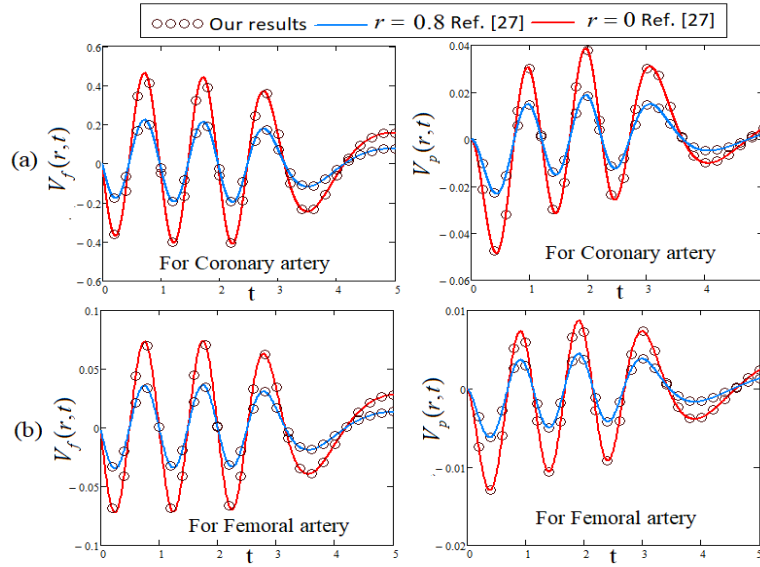


FIGURE 2. Response of velocity profiles versus t , varying r values for coronary and femoral artery

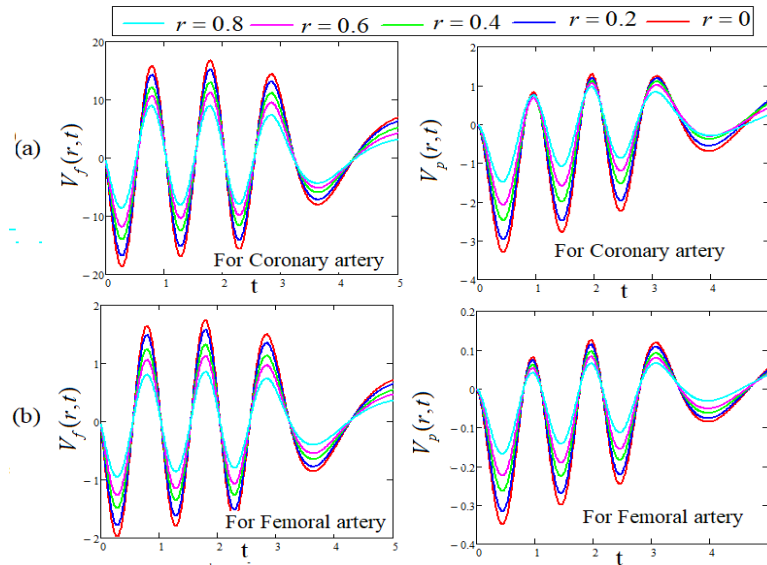


FIGURE 3. Response of velocity profiles versus t , varying r values for coronary and femoral artery.

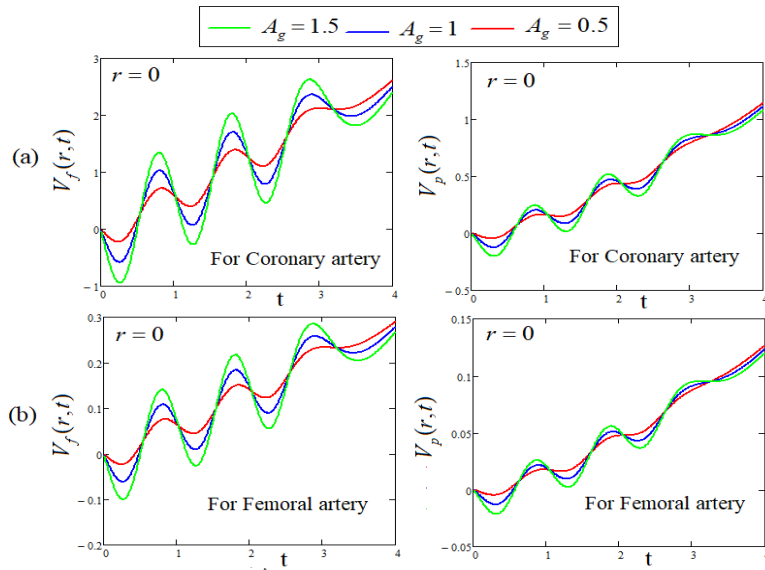


FIGURE 4. Response of velocity profiles versus time, varying A_g values for coronary and femoral arteries at $r = 0$

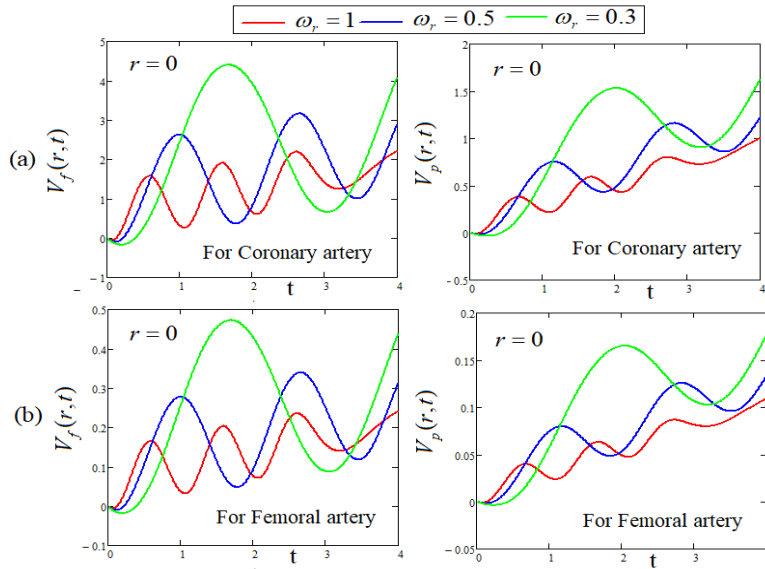


FIGURE 5. Response of velocity profiles versus time, varying ω_r values for coronary and femoral arteries at $r = 0$.

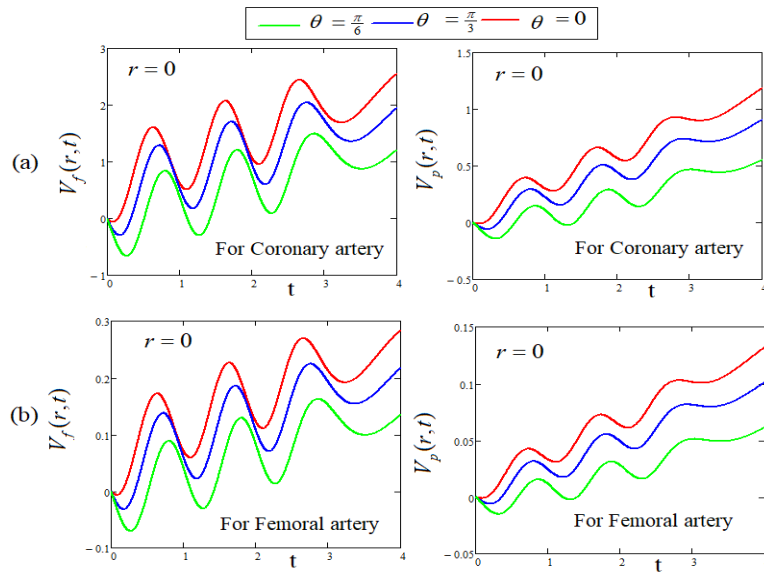


FIGURE 6. Response of velocity profiles versus time, varying θ values for coronary and femoral arteries at $r = 0$.

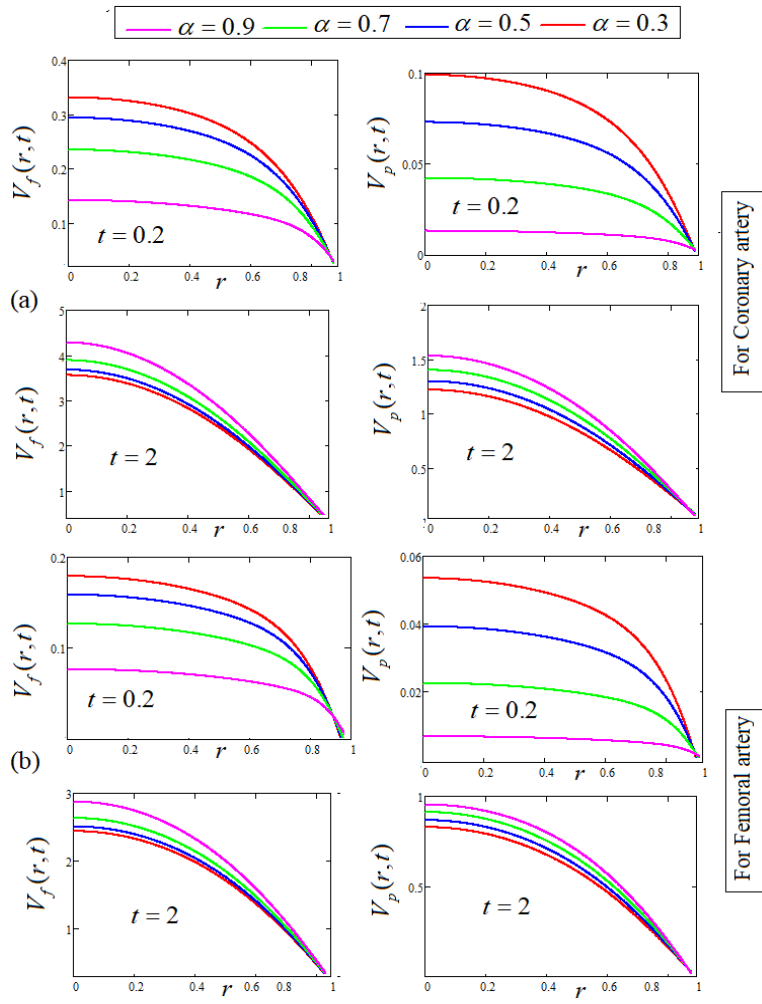


FIGURE 7. Response of velocity profiles versus r varying α values for coronary and femoral artery.

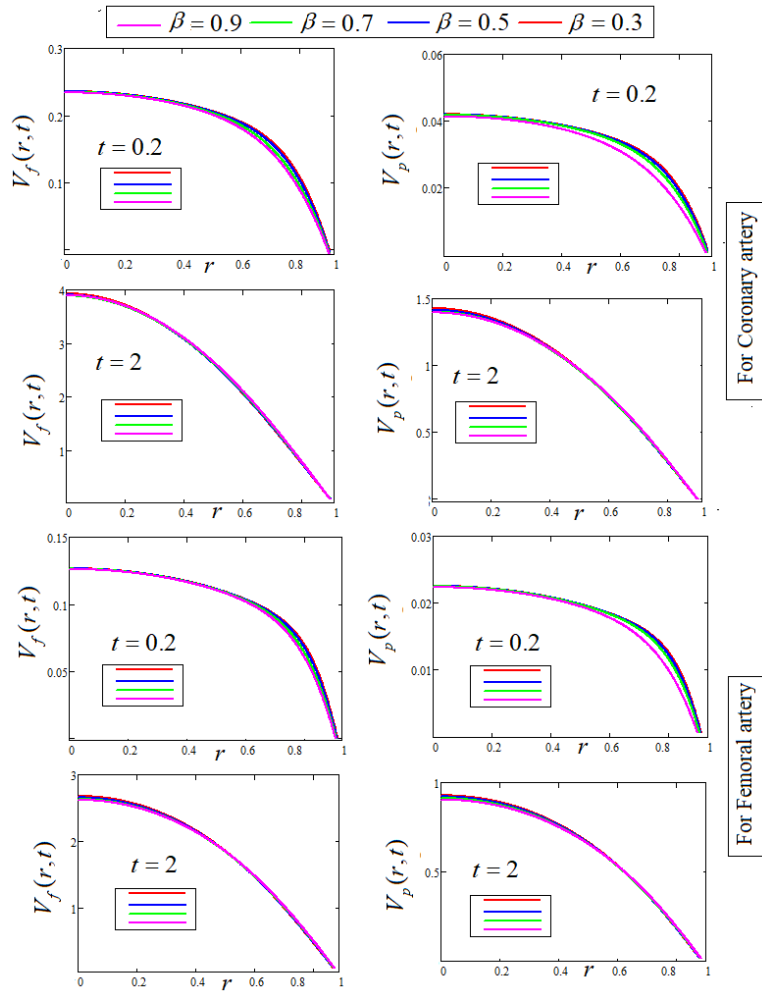


FIGURE 8. Response of velocity profiles versus r varying β values for coronary and femoral arteries at $t = 0.2$ and $t = 2$.

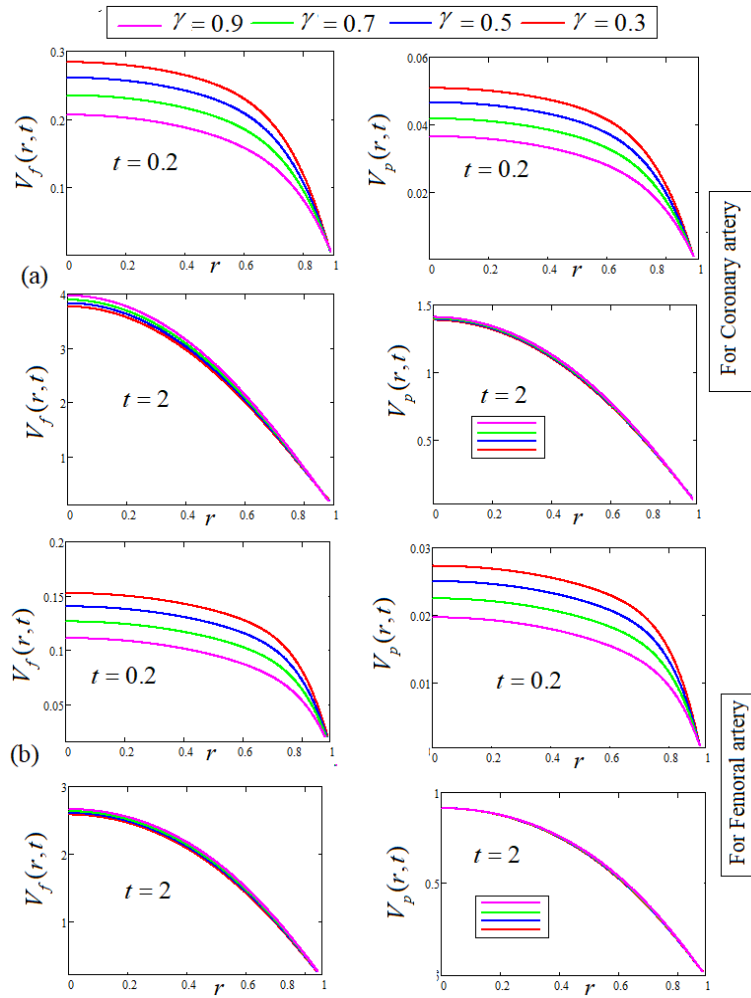


FIGURE 9. Response of velocity profiles versus r varying γ values for coronary and femoral arteries at $t = 0.2$ and $t = 2$.

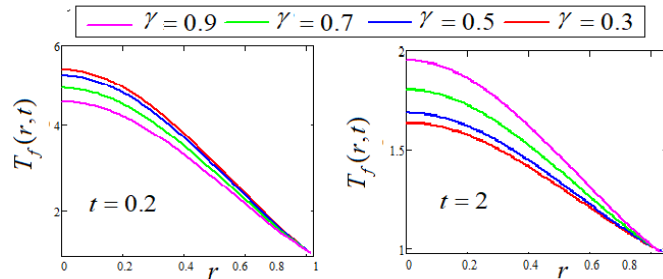


FIGURE 10. Response of temperature profiles versus r varying γ values at $t = 0.2$ and $t = 2$.

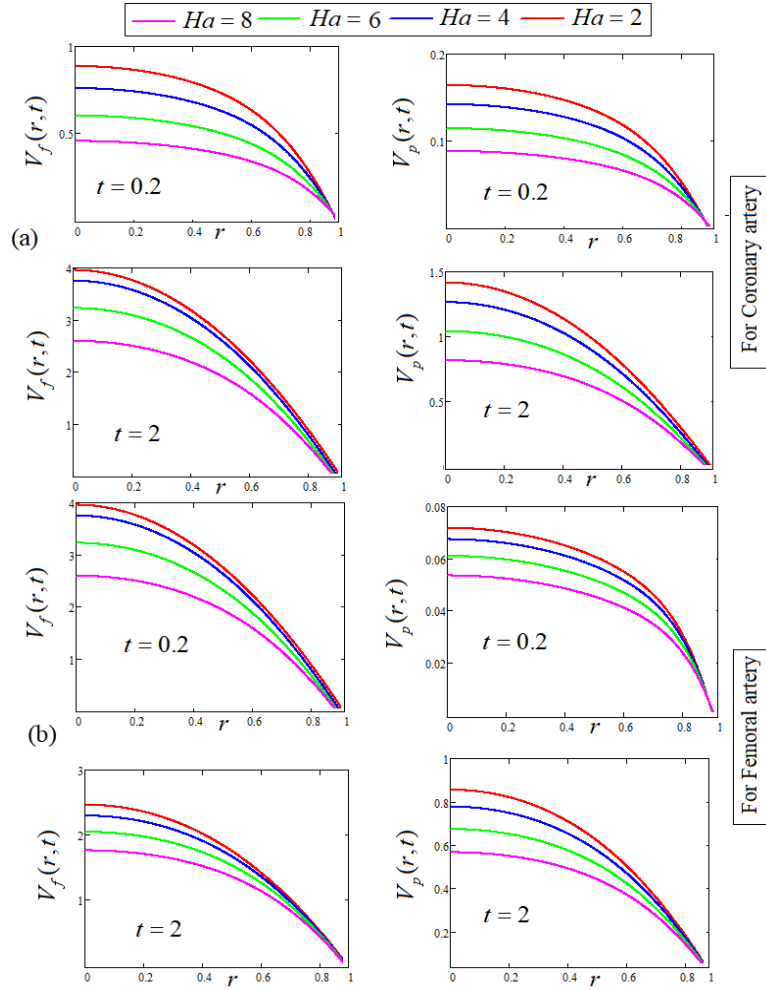


FIGURE 11. Response of velocity profiles versus r varying Ha values for coronary and femoral arteries at $t = 0.2$ and $t = 2$.

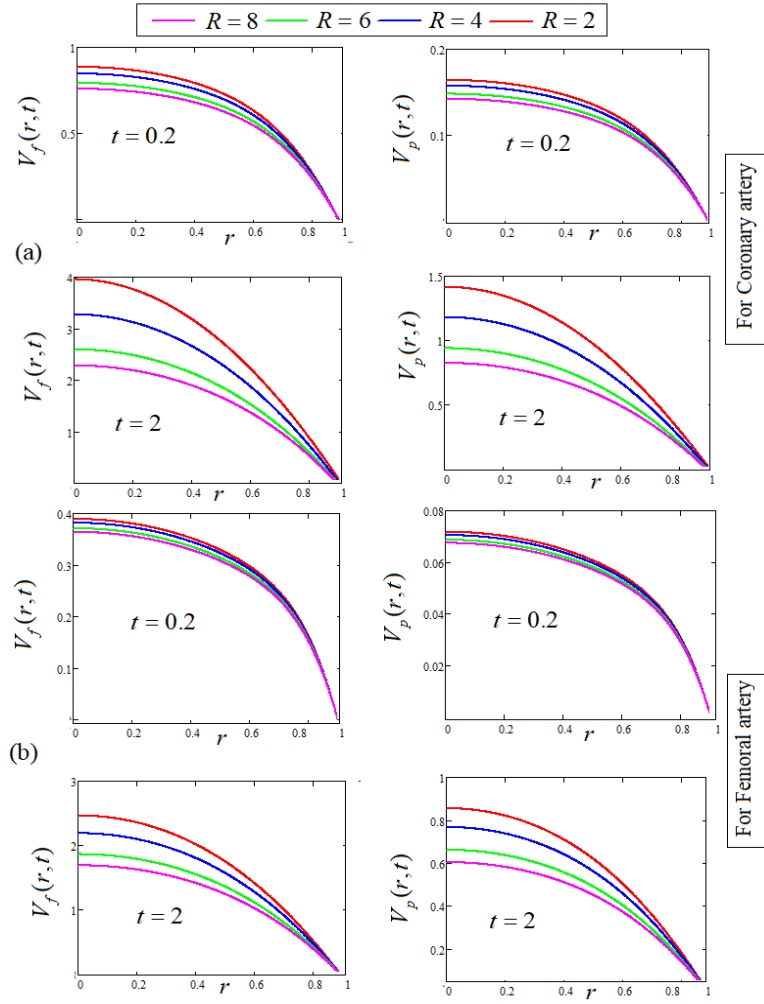


FIGURE 12. Response of velocity profiles versus r varying R values for coronary and femoral arteries at $t = 0.2$ and $t = 2$.

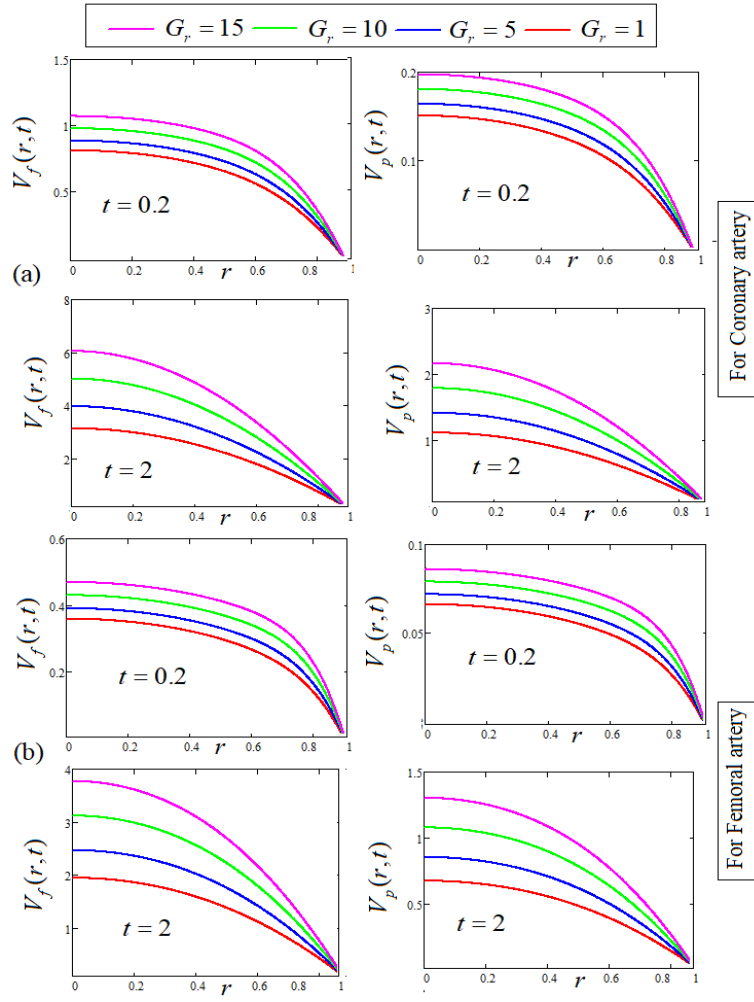


FIGURE 13. Response of velocity profiles versus r varying G_r values for coronary and femoral arteries at $t = 0.2$ and $t = 2$.

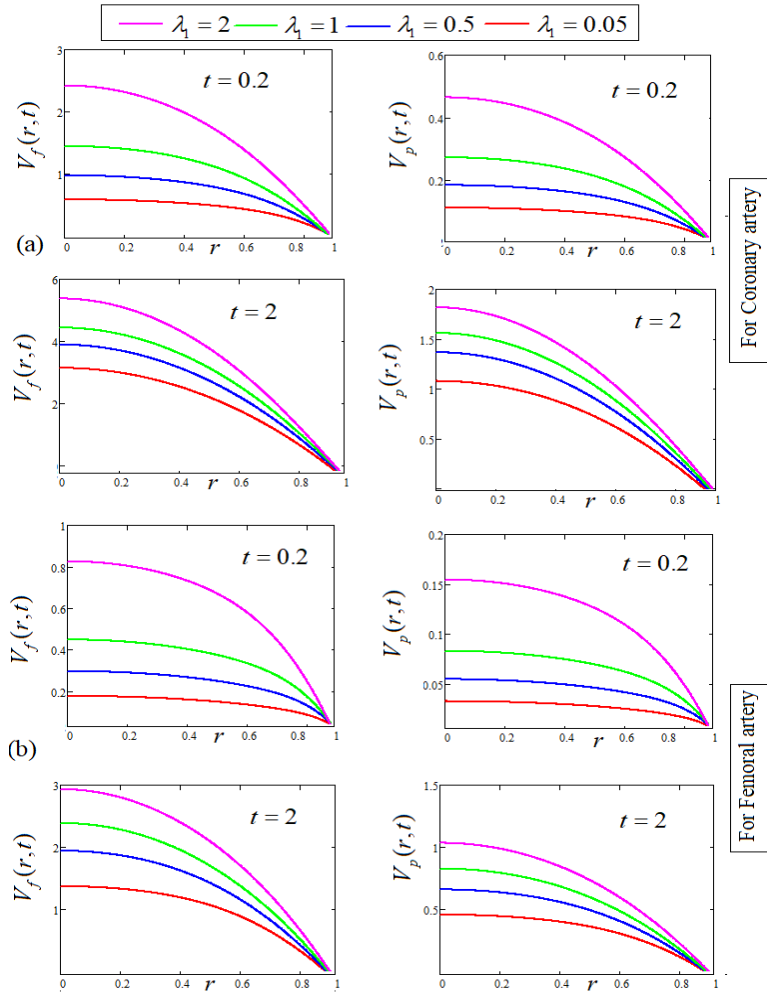


FIGURE 14. Response of velocity profiles versus r varying λ_1 values for coronary and femoral arteries at $t = 0.2$ and $t = 2$.

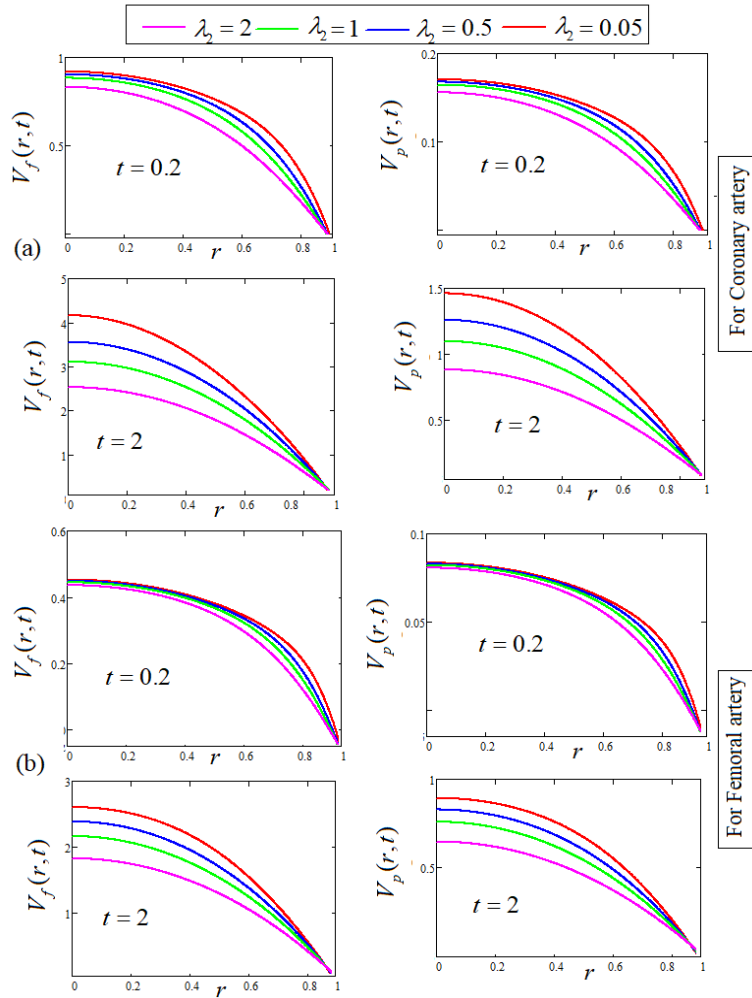


FIGURE 15. Response of velocity profiles versus r varying λ_2 values for coronary and femoral arteries at $t = 0.2$ and $t = 2$.

7. CONCLUSIONS

This study investigates blood flow non-integer order model in non-dimensional form subject to magnetic medium, incorporating factors such as transverse magnetic field, Stokes drag on distributed magnetic particles, and temperature effects. The circulation through the femoral and coronary arteries, driven by evenly suspended particles, is controlled by oscillatory pressure gradients and periodic body acceleration. The Oldroyd-B fluid model serves as the foundation for the governing equations, treating blood as a non-Newtonian

fluid. A fractional model is developed using the Atangana-Baleanu time fractional derivative. By combining finite Hankel and Laplace transformations, the study provides precise results for blood and suspended particles rheology.

- The Finite Hankel transform and Laplace transform were used to determine the exact solution.
- Observations of the memory-carrying parameter reveal distinct curves for velocity profiles at a fixed time, exhibiting dual behaviors over short and long periods.
- Blood velocity drops when Hartmann number rises.
- Higher amplitudes A_g of body acceleration in relation to cardiac activity result in an increase in blood flow velocity.
- Larger value of the lead angle θ and particles' concentration parameter R lead to decreased velocity of fluid and particles. The control of these parameters concerning coronary artery is prominent in contrary to femoral artery. Understanding these relationships is crucial to biomedical applications and can aid in the design of better therapeutic and diagnostic tools.
- In the femoral artery, ω_r has a stronger effect on blood and magnetic particle velocity than in the coronary artery
- λ_1 and λ_2 are the Oldroyd-B fluid parameters. As λ_1 increases, the velocity profile ascends but higher value of λ_2 results in a decreased velocity distribution.
- Larger value of the Grashof Number G_r leads to increased velocity of fluid and particles.

7.1. Final Thoughts. The consequences of this study are significant for biomedical science and clinical applications. The incorporation of a non-integer order model for blood flow using the Atangana-Baleanu fractional derivative provides a more nuanced understanding of blood rheology, capturing memory effects and complex behaviors not addressed in integer-order models. Moreover, the study demonstrates how various factors such as magnetic fields, body acceleration, particle concentration, and temperature influence blood and particle velocity. These findings can help in understanding hemodynamic responses under different physiological and pathological conditions. By identifying how parameters like Hartmann number, lead angle, and Grashof Number affect blood flow, the study offers insights that can be applied to optimize treatments such as targeted drug delivery and magnetic particle-based therapies. The distinct influence of body acceleration frequency on blood flow in the femoral and coronary arteries provide a basis for tailoring diagnostic tools for different arterial regions. The interplay between magnetic particles and fluid dynamics under external magnetic fields offers potential for developing better therapeutic strategies, such as magnetic hyperthermia or enhanced imaging techniques. Understanding how parameters like relaxation and retardation times of the Oldroyd-B fluid influence blood velocity can inform the design of medical devices, such as artificial pumps or stents, that mimic or support natural blood flow. The study's findings can aid in developing personalized treatment plans for conditions like arterial blockages or blood flow irregularities by allowing precise control of influencing factors. Overall, the study provides a comprehensive framework for analyzing blood flow behavior and opens avenues for innovative solutions in medical diagnostics and therapies.

8. FUTURE DIRECTIONS

In future studies, we plan to use other non-Newtonian models, such as the Sisko, Casson fluid models and incorporate different nano-particles, such as gold, and silver and give a comparative analysis of their fractional and non-fractional analogues with different fractional order operators. Moreover, due to the length of the manuscript, the graphs related to the influence of temperature are not included which would definitely be helpful in optimizing the cryosurgery, it would be incorporated in the future work.

AUTHOR CONTRIBUTIONS

Conceptualization, Azhar Ali Zafar and Muhammad Shahzaib; methodology, Khurram Shabbir and Azhar Ali Zafar; software, Muhammad Shahzaib.; validation, Azhar Ali Zafar, Khurram Shabbir and Muhammad Shahzaib; formal analysis, Azhar Ali Zafar; investigation, Azhar Ali Zafar; data curation, Muhammad Shahzaib; writing-original draft preparation, Azhar Ali Zafar and Muhammad Shahzaib; writing-review and editing, Khurram Shabbir; visualization, Azhar Ali Zafar; funding acquisition, Azhar Ali Zafar. All authors have read and agreed to the published version of the manuscript.

ACKNOWLEDGEMENTS

The authors would like to thank anonymous reviewers for their careful assessment and useful suggestions that helped us to improve the manuscript. Moreover, we are highly thankful and grateful to the Office of Research Innovation and Commercialization (ORIC), Government College University, Lahore, Pakistan, for generous support and facilitating this research work.

FUNDING

This work is the part of the ORIC funded faculty research project No. 422/ORIC/24 "Theoretical study of the rheology of biological fluids in human body in the presence of magnetic particles using fractional calculus modeling approach."

CONFLICTS OF INTEREST

The authors declare no conflict of interest.

REFERENCES

- [1] J. F. Aguilar, A. Atangana, *Fractional derivatives with the power law and the Mittag-Leffler kernel applied to the nonlinear Baggs-Freedman model*, *Fractal Fract.* **2**, No.10 (2018). <https://doi.org/10.3390/fractalfract2010010>.
- [2] F. Ali, A. Imtiaz, I. Khan, N. A. Sheikh, *Flow of magnetic particles in blood with isothermal heating: a fractional model for two-phase flow*, *J Magn Magn Mater.* No.456 (2018) 413422.
- [3] F. Ali, I. Khan, S. Ul Haq, S. Shafie, *Influence of thermal radiation on unsteady free convection MHD flow of Brinkman type fluid in a porous medium with Newtonian heating*, *Math Probl Eng.* (2013).
- [4] M. Alosaimi, I. Tekin, M. A. Cetin, *Restoration of the merely time-dependent lowest term in a linear Bi-flux diffusion equation*, *Computational and Applied Mathematics.* **43**, No.8 (2024). doi:10.1007/s40314-024-02937-7.
- [5] M.Alosaimi. I. Tekin, M. A. CETIN, *Simultaneous identification identification of the solely time dependent potential and source control*, *Mathematical Methods in the Applied Sciences.* **47**, No.7 (2023) 5532-5548.

- [6] A. Atangana, D. Baleanu, *New fractional derivatives with non-local and non-singular kernel: theory and applications to heat transfer model*, Thermal Sci. No.20 (2016) 763-769.
- [7] J. Awrejcewicz, A. A. Zafar, G. Kudra, M. B. Riaz, *Theoretical study of the blood flow in arteries in the presence of magnetic particles and under periodic body acceleration*, Chaos Solitons Fract. No.140 (2020) 110204. doi:10.1016/j.chaos.2020.110204.
- [8] D. Baleanu, A. Jajarmi, H. Mohammadi, S. Rezapour, *A new study on the mathematical modelling of human liver with Caputo-Fabrizio fractional derivative*, Chaos Soliton Fract. No.134 (2020) 109705.
- [9] R. B. Bird, W. E. Stewart, E. N. Lightfoot, *Transport Phenomena*, Wiley. (2002).
- [10] A. Bourhan, T. Magableh, *Magnetic field effect on heat transfer and fluid flow characteristics of blood flow in multi-stenosis arteries*, Heat Mass Transf. No.44 (2008) 297304.
- [11] P. J. Carreau, D. C. R. De Kee, R. P. Chhabra, *Rheology of Polymeric Systems: Principles and Applications*, Hanser Publishers. (1997).
- [12] P. Charles, E. Postow, *Handbook of biological effects of electromagnetic fields*, CRC Press (1996).
- [13] S. Chien, R. G. King, R. Skalak, S. Usami, A. L. Copley, *Viscoelastic properties of human blood and red cell suspension*, Biorheology. **12**, No.6 (1975) 341346.
- [14] L. Debnath, D. Bhatta, *Integral transforms and their applications*, 2nd Ed. Chapman and Hall, London, (2007).
- [15] A. D. Grief, G. Richardson, *Mathematical modelling of magnetically targeted drug delivery*, J Magn Magn Mater. **293**, No.1 (2005) 455463.
- [16] B. Gzik-Zroska, K. Jozsko, W. Wolanski, M. Gzik, *Development of new testing method of mechanical properties of porcine coronary arteries. Information technologies in medicine. In: Pietka E, Badura P, Kawa J, Wiclawek W (eds) 5th international conference, ITIB 2016, Kamien Slaski, Poland, 2022 June 2016, Proceedings*, Springer Cham. **2**, (2016) 289297.
- [17] Y. Haik, V. Pai, C. J. Chen, *Biomagnetic fluid dynamics at interfaces*, Cambridge, UK Cambridge University Press (1999).
- [18] J. Huang, R. Lyczkowski, D. Gidaspow, *Pulsatile flow in a coronary artery using multiphase kinetic theory*, J. Biomech. **42**, No.6 (2009) 743754.
- [19] M. Jawad, K. Shehzad, and R. Safdar. *Novel computational study on MHD flow of nanofluid flow with gyrotactic microorganism due to porous stretching sheet*. Punjab Univ. J. Math. **52**, No.12 (2021): 43-60.
- [20] C. Kilgus, A. Heidsieck, A. Ottersbach, W. Roell, C. Trueck, B. K. Fleischmann, P. Sasse, *Local gene targeting and cell positioning using magnetic nanoparticles and magnetic tips: comparison of mathematical simulations with experiments*, Pharm. Res. No.29, 13801391.
- [21] H. Khalil, R. A. Khan, M. H. Al-Smadi, A. A. Freihat. *Approximation of solution of time fractional order three-dimensional heat conduction problems with Jacobi Polynomials*. Punjab Univ. J. Math. **47**, no. 1(2020).
- [22] J. Liu, G. A. Flores, R. Sheng, *In-vitro investigation of blood embolization in cancer treatment using magnetorheological fluids*, J Magn Magn Mater. **225**, No.1-2,(2001) 209217.
- [23] C. F. Lorenzo, T. T. Hartley, *Generalized functions for fractional calculus*, Phys Rev. **8**, No.25 (2013) 11991204.
- [24] T. S. Lundgren, B. H. Atabek, C. C. Chang, *Transient magnetohydrodynamic duct flow*, Phys Fluids. **4**, No.8 (1961) 100611.
- [25] F. Mainardi, *Fractional calculus: some basic problems in continuum and statistical mechanics, Fractals and Fractional Calculus in Continuum Mechanics*, Springer, New York. (1997) 291348.
- [26] S. Maiti, S. Shaw, G. C. Shit, *CaputoFabrizio fractional order model on MHD blood flow with heat and mass transfer through a porous vessel in the presence of thermal radiation*, Physica A: Statistical Mechanics and its Applications, No.540 (2020) 123-149. doi: 10.1016/j.physa.2019.123149.
- [27] P. K. Mandal, *An unsteady analysis of non-Newtonian blood flow through tapered arteries with atherosclerosis*, Int J Nonlin Mech. **40**, No.1 (2005) 15164.
- [28] D. A. Mc Donald, *Blood flow in arteries*, London: Edward Arnold; (1974).
- [29] I. A. Mirza, M. Abdulhameed, S. Shafie, *Magnetohydrodynamic approach of non-Newtonian blood flow with magnetic particles in stenosed artery*, Appl. Math. Mech. **38**, No.3 (2017) 379392.
- [30] N. Mustapha, P. K. Mandal, P. R. Johnston, N. Amin, *A numerical simulation of unsteady blood flow through multi-irregular arterial stenosis*, Appl Math Model. **34**, No.6 (2010) 155973.
- [31] K. B. Oldham and J. Spanier, *The Fractional Calculus*, Academic Press, New York, (1974).

- [32] J. G. Oldroyd, *On the Formulation of Rheological Equations of Stat*, Proc. R. Soc., London, Ser. A. **200**, No.1063 (1950) 523541.
- [33] J. Plavins, M. Lauva, *Study of colloidal magnetite-binding erythrocytes: prospects for cell preparation*, J Magn Magn Mater. **122**, No.1-3 (1993) 349353.
- [34] M. B. Riaz, A. A. Zafar, *Exact solutions for the blood flow through a circular tube under the influence of a magnetic field using fractional Caputo-Fabrizio derivatives*, Math Model Nat Phenom. **13**, No.1 (2018) 8.
- [35] E. K. Ruuge, A. N. Rusetski, *Magnetic fluids as drug carriers: targeted transport of drugs by a magnetic field*, J Magn Magn Mater. **122**, No.1-3 (1993) 335339.
- [36] M. A. Sadiq Murad, and F. K. Hamasalh. Numerical study for fractional-order magnetohydrodynamic boundary layer fluid flow over stretching sheet. Punjab Univ. J. Math. 55, No. 2 (2023): 71-87.
- [37] S. S. Sajjadi, D. Baleanu, A. Jajarmi, H. M. Pirouz, *A new adaptive synchronization and hyperchaos control of a biological snap oscillator*, Chaos Soliton Fract. No.138 (2020) 109919.
- [38] N. A. Shah, D. Vieru, C. Feteacu, *Effects of the fractional order and magnetic field on the blood flow in cylindrical domains*, J Magn Magn Mater. No.409 (2016) 1019.
- [39] G. C. Shit, M. Roy, *Hydromagnetic pulsating flow of blood in a constricted porous channel: A theoretical study*, In Proceedings of the World Congress on Engineering, London, UK. **1**, (2012).
- [40] H. Stehfest, *Algorithm 368: Numerical Inversion of Laplace Transform*, Communications of the ACM. **13**, No.1 (1970) 47-49.
- [41] S. Tiari, M. Ahmadpour-B, M. Tafazzoli-Shadpour and M. R. Sadeghi, *An experimental study of blood flow in a model of coronary artery with single and double stenoses*, 2011 18th Iranian Conference of Biomedical Engineering (ICBME), Tehran, Iran, (2011) 33-36. doi: 10.1109/ICBME.2011.6168580.
- [42] G. B. Thurston, *Viscoelasticity of human blood*, J Biophys. **12**, No.9 (1972) 1205-1217.
- [43] G. B. Thurston, *Rheological parameters for the viscosity, viscoelasticity and Thixotropy of blood*, Biorheology. **16**, No.3 (1979) 149-162.
- [44] G. B. Thurston, N. M. Henderson, *The kinetics of viscoelastic changes due to blood clot formation*, Theoretical and Applied Rheology. No.112 (1992) 1721.
- [45] E. E. Tzirtzilakis, *A mathematical model for blood flow in magnetic field*, Phys Fluids **17**, No.7 (2005) .
- [46] V. K. G. Varshney, S. K. Kumar, *Effect of magnetic field on the blood flow in artery having multiple stenosis: a numerical study*, Int J Eng Sci Technol. **2**, No.2 (2010) 6782.
- [47] N. Westerhof, F. Bosman, C. J. De Vries, A. Noordergraaf, *Analog studies of the human systematic arterial tree*, J. Biomech. **2**, No.2 (1969) 121-143.
- [48] J. R. Womersley, *Method for the calculation of velocity, rate of flow and viscous drag in arteries when the pressure gradient is known*, Physiol J. **127**, No.3 (1955) 553-563.
- [49] K. K. Yeleswarapu, *Evaluation of continuum models for characterizing the constitutive behavior of blood*, Ph.D. thesis, University of Pittsburgh, (1996).
- [50] K. K. Yeleswarapu, M. V. Kamanava, K. R. Rajagopal, J. F. Antaki, *The flow of blood in tubes: Theory and experiment*, Mech Res Commun. **25**, No.3 (1998) 257262.
- [51] A. A. Zafar, N. A. Shah, I. Khan, *Two phase flow of blood through a circular tube with magnetic properties*, J Magn Magn Mater. No.477, (2019) 382387.